Pergamon

Tetrahedron 58 (2002) 727–739

TETRAHEDRON

Three-stranded mixed artificial β-sheets

James S. Nowick,* Eric M. Smith, Joseph W. Ziller and A. J. Shaka†

Department of Chemistry, University of California, Irvine, CA 92697-2025, USA

Received 16 July 2001; revised 13 September 2001; accepted 14 September 2001

Abstract—This paper describes the design, synthesis, and structural evaluation of a pair of compounds, comprising molecular templates and attached peptide strands, that mimic a small three-stranded mixed β-sheet (**6a** and **b**). Each of these artificial β-sheets is composed of two different molecular templates and two dipeptide strands. One of the templates is based on a 5-amino-2-methoxybenzoic hydrazide group that mimics the hydrogen-bonding functionality of a peptide β-strand and serves as the top strand. This template forms a pattern of hydrogen bonds similar to that of an antiparallel β-sheet with the middle peptide strand. The middle peptide strand forms a pattern of hydrogen bonds similar to that of a parallel β-sheet with the bottom peptide strand. The other template holds the three strands next to each other and is based upon a triurea. In one artificial β-sheet (**6a**), both the upper and middle urea groups and the middle and lower urea groups are linked by dimethylene (CH_2CH_2) chains; in the other (**6b**), the upper and middle urea groups are linked by a dimethylene chain, while the middle and lower urea groups are linked by a trimethylene ($CH_2CH_2CH_2$) chain. ^{1}H NMR chemical shift and NOE studies establish that both of these compounds fold to adopt a hydrogen-bonded β-sheetlike structure in $CDCl_3$ solution. Chemical shift studies establish that three-stranded mixed artificial β-sheets **6** are more tightly folded than their smaller two-stranded homologues, artificial parallel β-sheet **1** and artificial antiparallel β-sheet **3**, as well as their three-stranded homologues with truncated β-strand mimics, artificial β-sheets **5**. These studies show that the folding of artificial β-sheets **6** is cooperative, with the interactions between the upper and middle strands and between the middle and lower strands reinforcing each other.

Protein β-sheets come in two basic varieties—parallel and antiparallel. Parallel β-sheets are characterized by adjacent parallel peptide strands that form a series of twelve-membered hydrogen-bonded rings; antiparallel β-sheets are characterized by adjacent antiparallel peptide strands that form an alternating series of 10- and 14-membered hydrogen-bonded rings. Mixed β-sheets contain both parallel and antiparallel peptide strands with both types of hydrogen-bonding patterns. All of these structures occur widely in proteins, although mixed β-sheets are somewhat less common than antiparallel and parallel β-sheets.

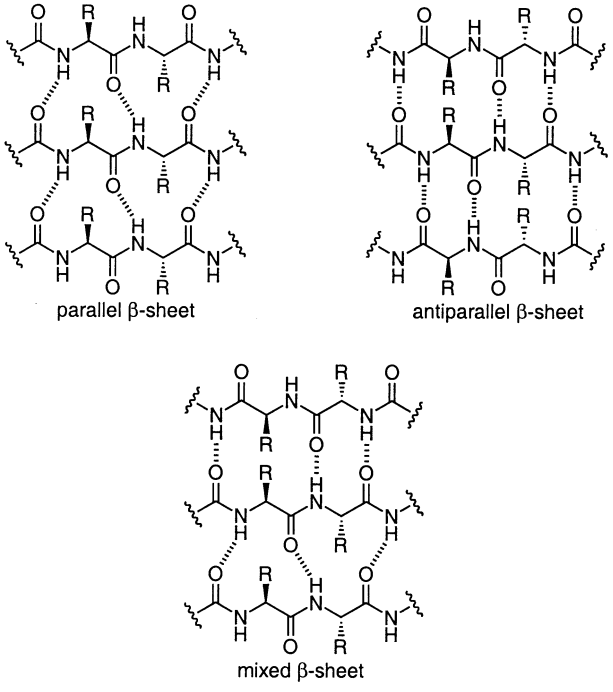

Researchers have developed a variety of small peptidelike molecules that fold to resemble protein β-sheets to gain enhanced understanding of protein folding and structure, invent new molecules and materials with proteinlike properties, and develop novel biologically active compounds. Pioneering efforts in this important and popular area have come from the research groups of Mutter,[1] Feigel,[2] Kemp,[3] Kelly,[4] Gellman,[5,6] and Seebach,[7,8] as well as from our own research group. These studies have lead to the creation of structures that resemble both antiparallel and parallel β-sheets. Related efforts have focused upon the creation of peptides that fold into antiparallel β-sheets,[9] with current studies focusing on the development of multistranded structures.[10]

While these efforts have yielded structures that resemble both parallel and antiparallel β-sheets, none, to our

Keywords: peptidomimetic; peptide; mixed beta sheets; molecular templates.

* Author to whom correspondence regarding synthetic and structural studies should be addressed. Fax: +1-949-824-8571;

† Author to whom correspondence regarding experimental NMR procedures should be addressed.
e-mail: jsnowick@uci.edu; ajshaka@uci.edu

0040–4020/02/$ - see front matter
PII: S0040-4020(01)01092-4

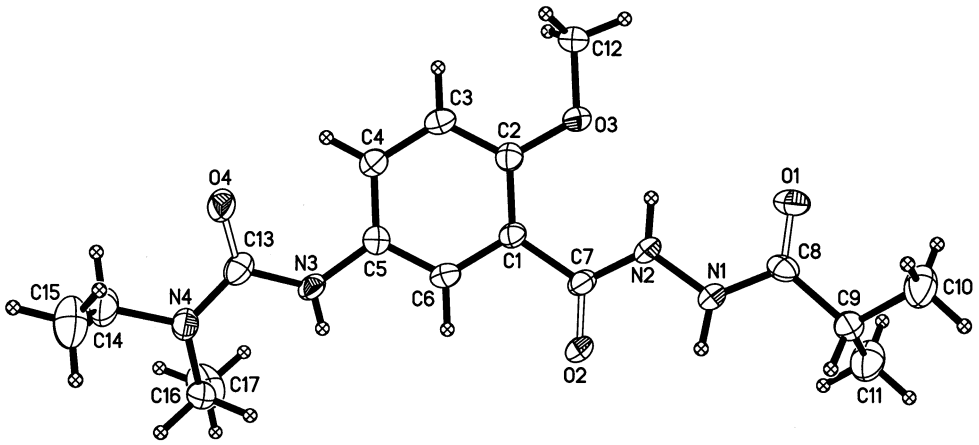

Figure 1. X-Ray crystallographic structure of 5-amino-2-methoxybenzoic hydrazide β-strand mimic **7**.

knowledge, have lead to structures that resemble mixed β-sheets. Our research group has actively been pursuing both parallel and antiparallel β-sheetlike structures since the early 1990s. We have termed these compounds, in which molecular templates induce β-sheet structure in attached peptide strands, *artificial* β-*sheets.* In 1995, we reported a small parallel artificial β-sheet (**1**) containing a diurea turn template that allowed the attachment of two peptide strands by their N-termini in a parallel fashion.[11] Shortly thereafter, we reported a series of two-stranded antiparallel β-sheets (e.g. **2** and **3**) containing the diurea turn structure and β-strand mimics designed to rigidify the sheet and block aggregation.[12] Concurrently, we reported a triurea homologue of the turn template (**4**) designed for the creation of three-stranded artificial β-sheets.[13] This work has paved the way for creating larger and more complex artificial β-sheets.[14] In the current study, we set out to determine whether we could create three-stranded mixed (parallel and antiparallel) artificial β-sheets by combining our triurea scaffold with two parallel peptide strands and a β-strand mimic.[15] This paper describes our design, synthesis, and evaluation of these structures.

1. Results and discussion

1.1. Design of three-stranded artificial β-sheets

We designed three-stranded mixed artificial β-sheets **6** based on our earlier studies of two-stranded artificial β-sheets **1** and **3** and triureas **4**. Artificial β-sheets **6** contain the same dipeptide groups (valylalanine and phenylalanylleucine) as artificial parallel β-sheet **1** and the same 5-amino-2-methoxybenzoic hydrazide β-strand mimic as artificial antiparallel β-sheet **3**. Artificial β-sheet **6a** contains a two-carbon linker between its lower and middle urea groups, while artificial β-sheet **6b** contains a three-carbon linker between these groups. We chose to evaluate both linkers, because X-ray crystallographic and molecular modeling studies raised concerns whether the shorter two-carbon linker would allow the lower peptide strand to properly align with the middle peptide strand in the three-stranded structures.[13] Previous studies in our laboratory had shown that while both two- and three-carbon linkers allowed oligoureas to form hydrogen-bonded turnlike structures, the two-carbon linked structures are more stably folded.[16,17]

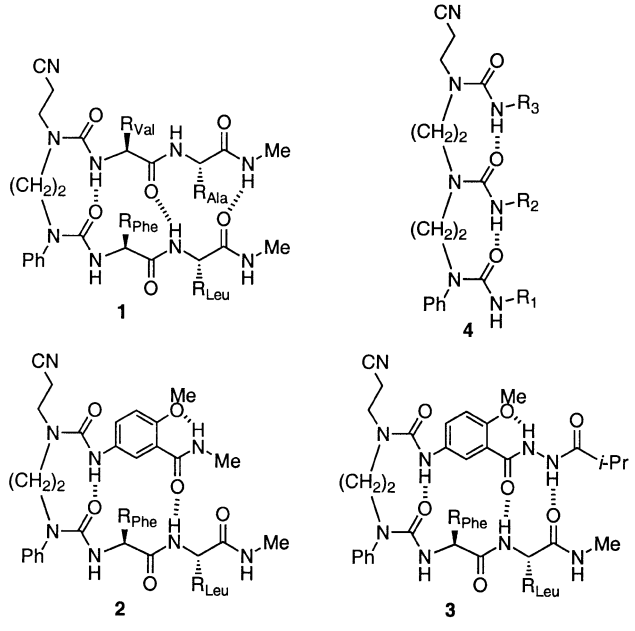

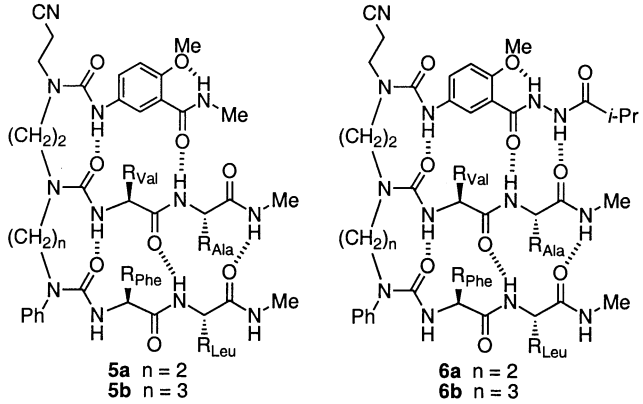

For comparison, we also designed artificial β-sheets **5**. These artificial β-sheets contain the truncated 5-amino-2-methoxybenzamide β-strand mimic that is present in artificial β-sheet **2**. The former β-strand mimic is long enough to hydrogen bond to the entire valylalanine dipeptide strand; the latter is only long enough to hydrogen bond to half of it. Like artificial β-sheets **6a** and **6b**, artificial β-sheet **5a**

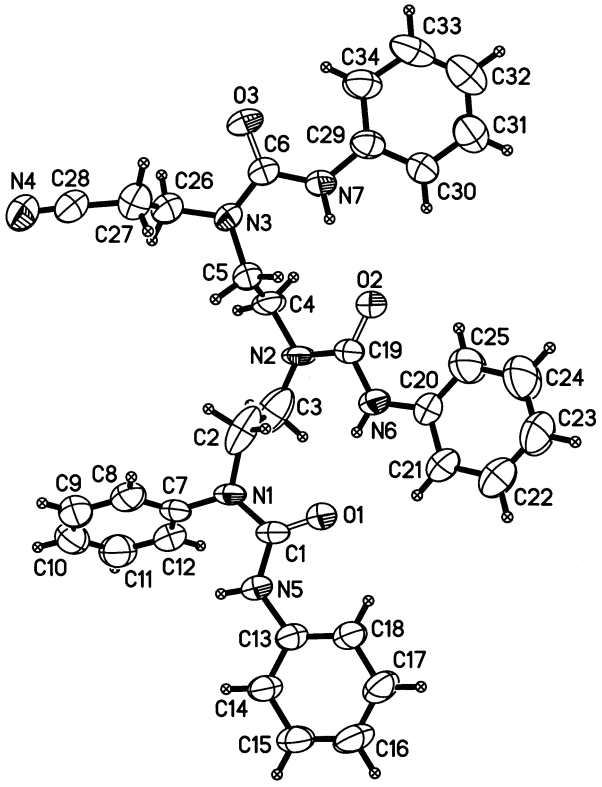

Figure 2. X-Ray crystallographic structure of triurea template **4a**.[13]

contains a two-carbon linker, and artificial β-sheet **5b** contains a three-carbon linker.

To gain insight into the structures of the β-strand mimic and triurea templates, we performed single-crystal X-ray crystallographic studies on simple crystalline compounds containing these building blocks.[18] Compound **7** contains the 5-amino-2-methoxybenzoic hydrazide β-strand mimic bearing a single urea group.[12c] X-Ray crystallography illustrates that it adopts an extended structure, with the urea, aromatic, and diacylhydrazine groups roughly coplanar (Fig. 1). This structure provides a linear arrangement of three hydrogen-bonding groups that can hydrogen bond to a tripeptide. We have previously reported the X-ray crystallographic structures of triureas **4a** (R_1, R_2, R_3=Ph) and **4b** (R_1, R_2, R_3=Me).[13] (The structure of **4a** is reproduced here in Fig. 2.) These studies have shown that the three urea groups hydrogen bond together and align the substituents

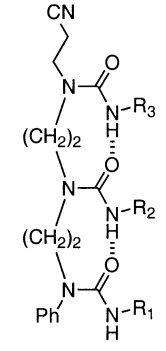

4a R_1, R_2, R_3 = Ph
4b R_1, R_2, R_3 = Me

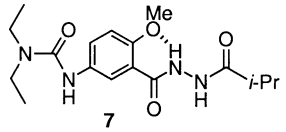

7

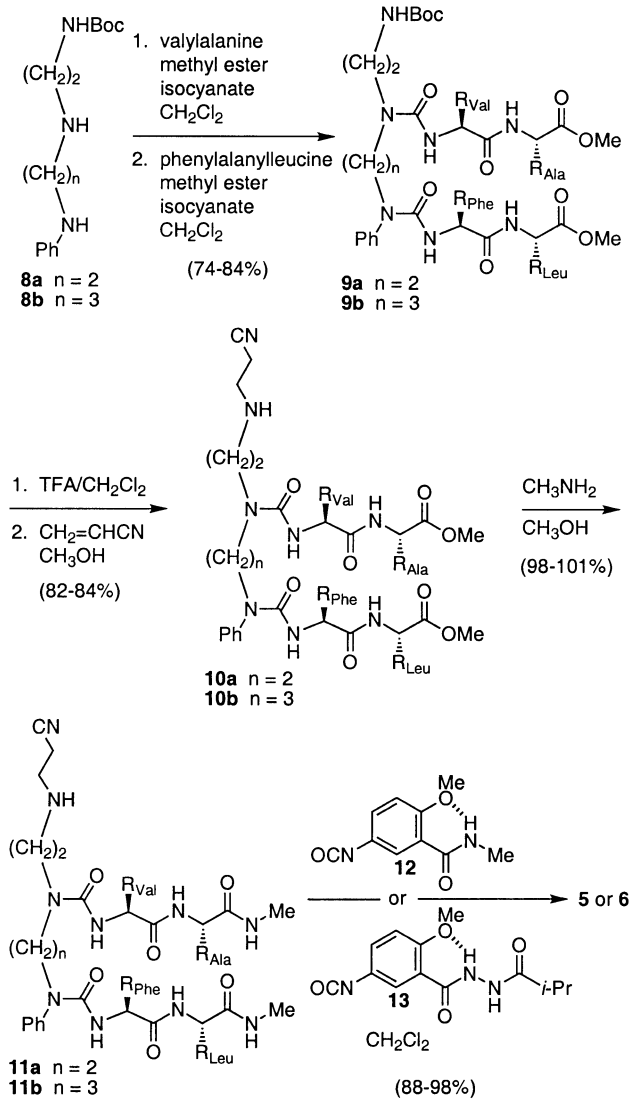

Scheme 1.

R_1–R_3 in roughly the right orientation to allow β-sheet formation.

1.2. Synthesis of artificial β-sheets 5 and 6

Artificial β-sheets **5** and **6** were efficiently synthesized from diamines **8**[13] by the procedures we reported previously for the synthesis of triureas **4**.[19] Artificial β-sheets **5a** and **6a** were prepared from diamine **8a**, which contains a two-carbon linker between its amino groups; artificial β-sheets **5b** and **6b** were prepared from diamine **8b**, which contains a three-carbon linker. Scheme 1 illustrates their syntheses.

Diamines **8a** and **b** were converted to diureas **9a** and **b** by treatment first with 1 equiv. of valylalanine methyl ester isocyanate and then with a second equivalent of phenylalanylleucine methyl ester isocyanate.[20] The reactions of diamines **8a** and **b** with the isocyanates are highly regioselective, because the amino group at the middle position is aliphatic and is relatively reactive, while the amino group at the bottom position is aromatic and is less reactive.[13] A third amino group, at the top position, is protected as the Boc

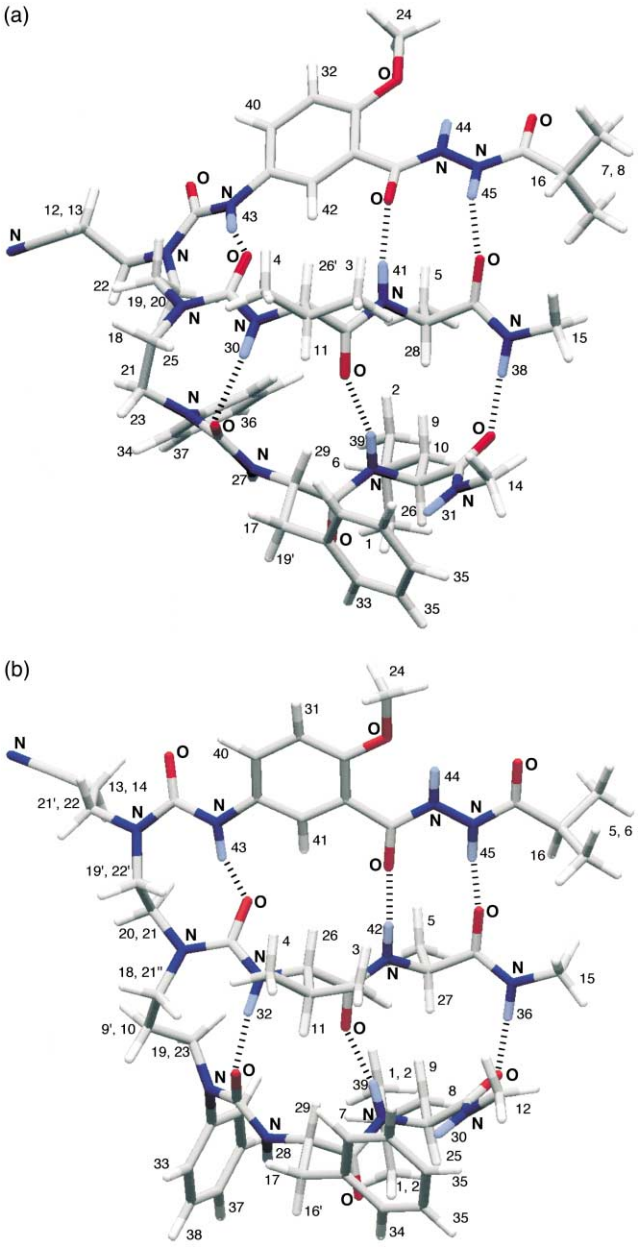

Figure 3. Models of artificial β-sheets **6a** and **6b** showing the assignments of the 500 MHz ^{1}H NMR spectral resonances of the compounds in 25 mM $CDCl_3$ at 298 K. The models were generated using MacroModel V5.0 with the AMBER* force field. The starting conformations (before minimization) of the amino acid side-chains were chosen to reflect measured coupling constants and NOEs when possible, but are largely arbitrary. The spectral resonances for each compound were numbered 1–45, from upfield (low ppm) to downfield (high ppm).

derivative and is not reactive. The Boc protective groups of **9a** and **b** were removed by treatment with trifluoroacetic acid (TFA), and the resulting primary amines were cyanoethylated with acrylonitrile to form secondary amines **10a** and **b**. The methyl ester groups of **10a** and **b** were converted to methylamide groups by aminolysis with methylamine in methanol, affording secondary diamides **11a** and **b**. Reaction of **11a** and **b** with isocyanate **12**[15a] afforded artificial β-sheets **5a** and **b**, while reaction of **11a** and **b** with isocyanate **13**[15a] afforded artificial β-sheets **6a** and **b**.

1.3. ^{1}H NMR spectroscopic characterization and assignment of artificial β-sheets 6

Artificial β-sheets **6a** and **6b** were thoroughly characterized by ^{1}H NMR spectroscopy in $CDCl_3$ solution. First, the one-dimensional spectra of these compounds were recorded at 500 MHz. The resonances were then numbered sequentially, beginning at the upfield region of the spectra, and tabulated. When resonances were subsequently identified to comprise a group of overlapping peaks, prime (′) and double-prime (″) designations were added to the numbers to reflect the individual components of the peaks. Two-dimensional PFG-COSY and Tr-ROESY[21] spectra were then recorded and used to assign the resonances. Molecular modeling was used to aid in the assignments of resonances from diastereotopic methyl and methylene groups and guide the analysis of the Tr-ROESY data. Molecular models of **6a** and **6b** were generated using MacroModel V5.0 with the AMBER* force field.[22] The starting conformations (before minimization) of the amino acid side-chains were chosen to reflect measured coupling constants and NOEs when possible, but are largely arbitrary. Fig. 3a and b show these molecular models and the assignments of the resonances to their respective protons.

On the basis of these models and the NOE and coupling constant data, the diastereotopic methyl and methylene resonances for the valine and phenylalanine side chains of both **6a** and **6b** were assigned with reasonable confidence. The diastereotopic leucine methylene resonances of **6a** and **6b** were also assigned with reasonable confidence, as were the leucine methyl resonances of **6a**. Assignments of the diastereotopic methylene resonances of the triamine backbones of **6a** and **6b** were not possible, with the exception of the lower dimethylene group of **6a** ($PhNCH_2CH_2N$). Analysis of the coupling constants and NOEs associated with this group strongly suggested it to adopt a single *gauche* conformation (shown in Fig. 3a).

1.4. ^{1}H NMR NOE studies of artificial β-sheets 6

The Tr-ROESY studies described earlier provide strong evidence that artificial β-sheets **6a** and **6b** fold into β-sheet-like structures. Most compelling among the data is an extensive network of NOEs between the β-strand mimic (upper strand) and the valylalanine dipeptide group (middle strand) and between the valylalanine dipeptide group and the phenylalanyl dipeptide group (lower strand) in both compounds.[23] Both artificial β-sheets **6a** and **6b** exhibit NOEs between the 6-position of the aromatic ring of the β-strand mimic and the valine α-proton and alanine side chain, the hydrazide NH_i proton and the alanine methyl group, the isobutyryl methyl groups and alanine methylamide methyl group, the phenylalanine α-proton and the valine NH and side chain, the phenylalanine side chain and the valine side chain, the alanine α-proton and the leucine NH and side chain, and the alanine methylamide NH group and the leucine methylamide methyl group. Chart 1 succinctly shows these NOEs with arrows.

A number of minor differences among the interstrand NOEs observed for the two compounds are present. Artificial β-sheet **6a** exhibits an NOE between the alanine and leucine

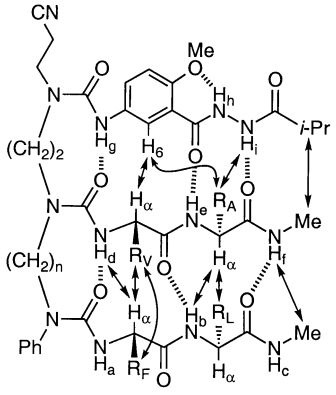

Chart 1.

side chains and between the alanine and leucine α-protons; artificial β-sheet **6b** exhibits an NOE between the hydrazide NH_i proton and the alanine NH group, and between the phenylalanine side chain and the alanine methylamide methyl group. These differing NOEs are generally weak and may reflect small differences in the conformations or conformational populations of the two compounds. The presence of a weak NOE between the alanine and leucine α-protons of **6a** may, for example, indicate small deviation from ideal β-sheetlike structure. The presence of a weak to moderate NOE between the phenylalanine side chain and the alanine methylamide methyl group in **6b** may reflect conformations in which the molecule twists in the fashion characteristic of β-sheets to bring these groups into proximity. While these differences in observed NOEs may reflect meaningful conformational differences, it is also possible that they merely reflect insignificant differences between the signal-to-noise levels of the Tr-ROESY experiments on the two compounds.

Intrastrand NOEs between the NH and α-protons of the valylalanine peptide strand of **6a** and **6b** suggest that this peptide strand adopts a β-strandlike conformation in both compounds.[23] Thus, this peptide strand shows strong interresidue NOEs between the NH and α-protons and weaker intraresidue NOEs between the NH and α-protons in both compounds. In a similar fashion, the upper β-strand mimic shows a relatively strong NOE between the NH proton H_g and the proton at its 6-position and little or no NOE between

Table 1. ^{1}H NMR chemical shifts of the NH protons of **1**–**3**, **5**–**7**, and **14**–**18**

	H_a	H_b	H_c	H_d	H_e	H_f	H_g	H_h	H_i
1	4.61	7.37	6.23	6.68	6.75	6.96			
2	5.02	8.20	5.45				10.00	8.11	
3	4.82	8.29	5.79				9.93	10.97	10.45
5a	4.62	7.16	6.53	6.57	8.46	7.00	9.98	8.14	
5b	4.67	7.03	6.27	6.27	8.41	6.84	10.05	8.13	
6a	4.38	8.16	6.72	6.17	8.53	7.94	10.01	10.87	11.07
6b	4.75	8.22	5.87	6.96	8.79	7.36	10.42	11.04	11.22
7							6.31	10.85	8.78
14							6.31	7.92	
15				4.75	6.34	6.58			
16					6.01	6.01			
17	4.43	6.37	6.71						
18		5.82	6.00						

Spectra were recorded at 295 K in 1.0 mM $CDCl_3$ solution.

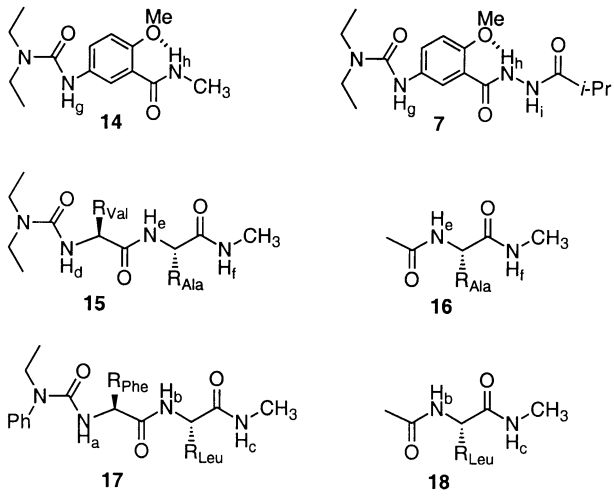

Chart 2.

this NH proton and the proton at its 4-position in both **6a** and **6b**. The intraresidue and interresidue NOEs between the NH and α-protons of the phenylalanylleucine peptide strand are comparable in strength in both compounds, suggesting that the conformation of this strand is less β-strandlike than the valylalanine peptide strand. The $^3J_{HN\alpha}$ coupling constants of the four amino acids in both compounds are consistent with β-strandlike conformations, ranging from 8.3–9.3 Hz.[24] Collectively, these NOE and coupling constant data support a model in which both **6a** and **6b** adopt structures that are basically β-sheetlike, with minor deviation from β-sheetlike structure occurring in the lower peptide strand.

1.5. ^{1}H NMR chemical shift studies of artificial β-sheets 6

Comparison of the ^{1}H NMR chemical shifts of the NH groups of artificial β-sheets **6** to appropriate non-β-sheetlike controls provides quantitative insight into their folding. In $CDCl_3$ solution, non-hydrogen-bonded peptide amide protons resonate at about 6 ppm and non-hydrogen-bonded peptide urea protons resonate at about 4.5 ppm.[11,16,17] When hydrogen bonded, these protons resonate ca. 2–2.5 ppm further downfield.[11,16,17] A fully hydrogen-bonded peptide amide proton typically appears slightly downfield of 8 ppm; a fully hydrogen-bonded peptide urea proton typically appears at ca. 7 ppm. Amide and urea protons that are in rapid equilibrium between hydrogen-bonded and non-hydrogen-bonded states or are weakly hydrogen bonded appear at intermediate chemical shifts. Other types of NH protons (e.g. aromatic ureas and hydrazides) appear at different positions and also shift downfield upon hydrogen bonding, with their degree of downfield shifting roughly reflecting their degree of hydrogen bonding.

For these studies, the chemical shifts of artificial β-sheets **6** were recorded at 1.0 mM in $CDCl_3$ at 295 K and compared to controls **7** and **15**–**18**.[25] Control **7** resembles the β-strand mimic (upper strand) of **6**.[12c] Controls **15** and **16** respectively resemble the entire middle (valylalanine) peptide strand and the right-hand portion of this peptide strand; controls **17** and **18** respectively resemble the entire lower (phenylalanylleucine) peptide strand and the right-hand portion of this peptide strand.[11,12a] Two compounds are

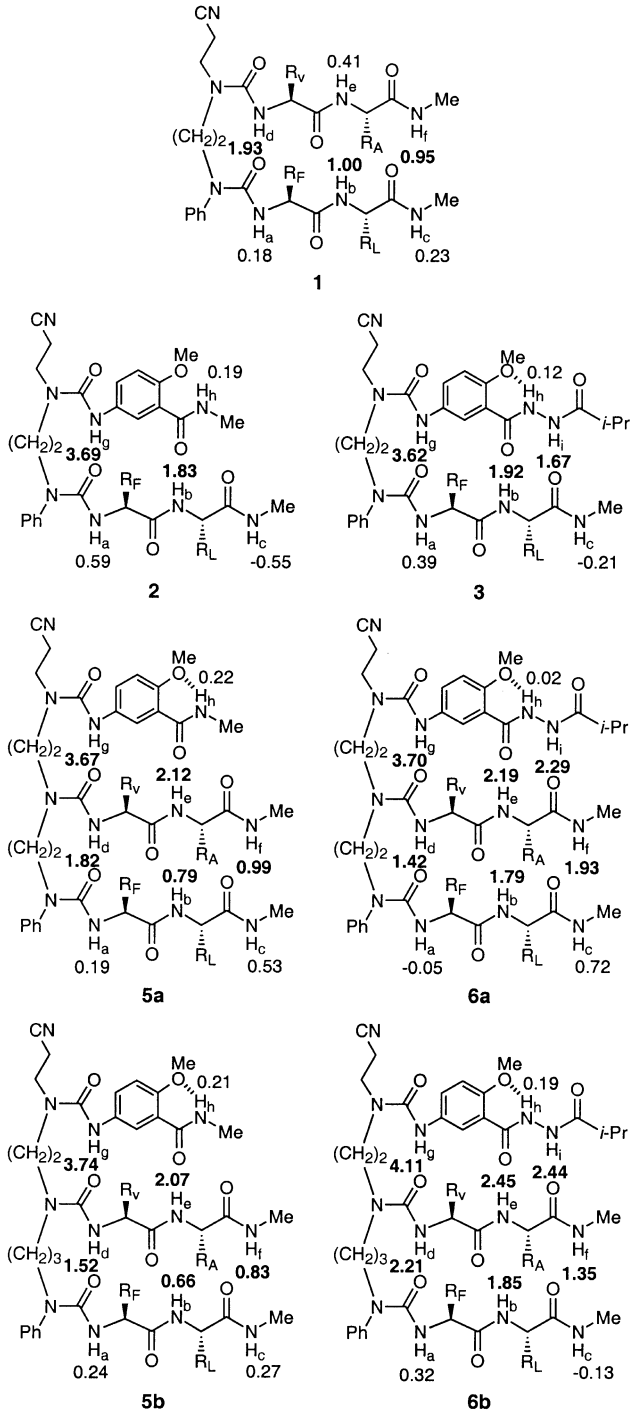

Chart 3.

used as controls for each of the peptide strands, because the longer compounds tend to adopt β-turnlike conformations in which the methylamide NH groups are hydrogen bonded to the urea carbonyl groups. Thus, the shorter compounds serve as better controls for the methylamide NH groups. Table 1 summarizes the chemical shifts of the NH resonances of these compounds. Also included are shift data for artificial β-sheets **1**–**3**, and **5** and control **14**, which are discussed subsequently.[11,12a,c] Chart 2 shows the assignments of these resonances to their respective protons, which are designated H_a–H_i.

Comparison of the chemical shifts of the NH groups of artificial β-sheets **6a** and **6b** to those of controls **7** and **15**–**18** indicates that protons H_b, H_d–H_g, and H_i are largely or wholly hydrogen bonded while protons H_a and H_c are largely not hydrogen bonded. Chart 3 summarizes these chemical shift differences and also shows the chemical shift differences between artificial β-sheets **1**–**3** and **5** and the corresponding controls, which are discussed subsequently. In artificial β-sheets **6a** and **6b**, protons H_b, H_e, and H_i appear 1.79–2.45 ppm downfield of their respective controls, indicating that they are largely or wholly hydrogen bonded. Proton H_d appears 2.21 ppm downfield of control **15** in artificial β-sheet **6b** but only 1.42 ppm downfield in artificial β-sheet **6a**. This unusually small downfield shifting may reflect that the NH group in this compound must hydrogen bond to the π-face of the carbonyl, rather than to the lone pair of electrons, to allow the lower dimethylene group of **6a** ($PhNCH_2CH_2N$) to adopt a *gauche* conformation (discussed earlier and shown in Fig. 3a).

Proton H_f appears 1.93 ppm downfield of control **16** in artificial β-sheet **6a** but only 1.35 ppm downfield in artificial β-sheet **6b**. The unusually small downfield shifting of this proton in **6b** suggests that it is hydrogen bonded slightly more than half of the time and may reflect some fraying of the lower right-hand corner of the β-sheet. This deviation in shift mirrors some of the variations observed in the intra- and interresidue NOEs, discussed earlier.

Proton H_g appears exceptionally far (3.70–4.41 ppm) downfield of control **7** in artificial β-sheets **6**. The unusually large downfield shifting of this proton may result from anisotropic effects associated with changes in the torsion angle about the bond between the urea group and the aromatic ring of the β-strand mimic or may reflect an exceptionally strong hydrogen bond in which the carbonyl group of the middle urea is jammed into the NH_g group of the upper urea.[12a] Proton H_a appears within −0.05–0.32 ppm of control **17**, indicating it to not be significantly hydrogen bonded in either compound. Proton H_c appears within −0.13 ppm of control **18** in artificial β-sheet **6b**, while it appears 0.72 ppm downfield of this control in artificial β-sheet **6a**. This downfield shifting of H_c in **6a** provides further evidence for the bottom peptide strand's partial deviation from β-sheetlike structure in this compound. Proton H_h, which is hydrogen bonded in control **7**, is also hydrogen bonded in artificial β-sheets **6** and appears at nearly the same chemical shifts in all three compounds.

1.6. Comparison of artificial β-sheets 6 to other artificial β-sheets

Comparison of the ^1H NMR chemical shifts of the NH protons of artificial β-sheets **6** to those of artificial β-sheets **1** and **5** provides insight into the effects of the β-strand mimic upon the structure of **6**. Two-stranded artificial β-sheet **1** contains the two peptide strands that are present in **6** with a two-carbon linker (like **6a**). Three-stranded artificial β-sheets **5a** and **5b** contain the same two peptide strands and a truncated version of the β-strand mimic that lacks the hydrogen-bond donor (NH_i) of the hydrazide group. Chart 3 provides a convenient comparison of the downfield shifting of the NH protons in these compounds

relative to controls. Chart 3 also provides a comparison to two-stranded artificial β-sheets **2** and **3**, which are smaller homologues of **5** and **6** that contain the same β-strand mimics and phenylalanylleucine peptide strand but lack the middle valylalanine peptide strand.

Particularly notable is that protons H_b and H_f are shifted much further downfield in **6a** and **6b** than in **5a** and **5b** or in **1**. In **6a**, H_b and H_f appear 1.79 and 1.93 ppm downfield of the corresponding protons in controls **17** and **16**; in **6b** H_b and H_f appear 1.85 and 1.35 ppm downfield. In **5a**, H_b and H_f appear only 0.79 and 0.99 ppm downfield; in **5b**, these protons appear only 0.66 and 0.83 ppm downfield. In **1**, they appear 1.00 and 0.95 ppm downfield. The downfield shifting of these protons suggests that the peptide strands of artificial β-sheets **6** are largely hydrogen bonded while those of **1** and **5** are a little less than half hydrogen bonded (assuming a dynamic equilibrium in which 2–2.5 ppm downfield shifting corresponds to complete hydrogen bonding).

Also notable is that H_i is shifted further downfield in **6a** and **6b** than in **3**. In **6a** and **6b**, H_i appears 2.29–2.44 ppm downfield of the corresponding proton in control **7**, while in **3**, H_i appears only 1.67 ppm downfield. This greater degree of downfield shifting suggests more complete hydrogen bonding between the upper and middle strands of three-stranded artificial β-sheets **6** than between the strands of two-stranded artificial β-sheet **3**. Further support for the greater degree of folding of the three stranded structures comes from comparison of the downfield shifting of the alanine NH_e proton in artificial β-sheets **5** and **6** to the downfield shifting of the leucine NH_b proton in artificial β-sheets **2** and **3**. In artificial β-sheets **5** and **6**, H_e appears 2.07–2.45 ppm downfield of the corresponding proton in control **15**, while in **2** and **3**, H_b appears only 1.83–1.92 ppm downfield of the corresponding proton in control **17**. This comparison is fairly reasonable, because the spatial relationship of the protons (H_e and H_b) to the β-strand mimics of the different compounds is the same, even though they belong to different amino acid residues.[26]

Together, these data indicate that artificial β-sheets **6** are more completely folded than artificial β-sheets **1**, **3**, or **5**. The lower two peptide strands of **6** are more thoroughly paired than the two peptide strands in **1**, the upper two strands of **6** are more thoroughly paired than the two strands in **3**, and the fully templated three-stranded structure of **6** is better folded than the partially templated three-stranded structure of **5**. That artificial β-sheets **6** are better folded than artificial β-sheets **1**, **3**, or **5** indicates that the folding of **6** is cooperative. These findings of cooperativity in this mixed β-sheet system match the findings of cooperativity in the folding of three-stranded antiparallel peptide β-sheets by the groups of Searle,[10a,i] Gellman,[10c] and Kortemme and Ramírez-Alvarado.[10e]

The current studies do not establish whether the extra stability of **6** arises only because of cooperativity, or whether the relatively rigid β-strand mimic of **6** also imparts extra stability beyond that which would be provided by a third peptide strand. A comparison of artificial β-sheets **1** and **3** suggests that the β-strand mimic does impart some special stability associated with its preorganization in a β-strandlike conformation. Most notably, the leucine NH_b proton of **3** appears 1.92 ppm downfield of the corresponding proton in control **17**, while in **1** it appears only 1.00 ppm downfield. Protons H_g and H_i in **3** are also more strongly shifted downfield of their respective controls than are the spatially related protons H_d and H_f in **1**, however these protons differ too much in environment and type to allow meaningful comparison.

2. Conclusion

These synthetic and structural studies establish a paradigm for the creation of small peptidelike molecules that fold in chloroform solution to resemble three-stranded mixed β-sheets. Central to this paradigm is the use of a triurea molecular scaffold to hold the three strands next to each other in suitable orientations. The middle and lower strands are peptides and are attached at their N-termini, while the upper strand is a peptidomimetic template that resembles a peptide β-strand that is attached by its C-terminus. The β-strand mimic may be viewed as acting in conjunction with the triurea template to form a 'corner bracket' that stabilizes β-sheet structure in both of the attached peptide strands, and the folding of the artificial β-sheets may be viewed as being cooperative, with the β-strand mimic helping to organize the middle peptide strand in a β-strand-like conformation and thus augmenting its interaction with the lower peptide strand.

Although substantial differences between the three-stranded mixed artificial β-sheets containing two- and three-carbon linkers between the lower and middle urea groups were anticipated, only minor differences were found. Both the two- and three-carbon linkers afford artificial β-sheets in which the middle peptide strand is well ordered and the lower peptide strand is slightly less ordered. While the peptide strands in the current study are relatively short (dipeptides), previous studies in our laboratories have shown that it is possible to prepare two-stranded artificial β-sheets containing longer peptide strands and extended versions of the β-strand mimic or the β-strand mimic linked to a peptide.[12b,d] The preparation of three-stranded mixed artificial β-sheets containing longer strands such as these should also be possible. Collectively, these studies show that our modular approach to the creation of structures that fold to resemble protein β-sheets is robust and pave the way for even larger and more complex structures that mimic the complex topologies of proteins.

3. Experimental

3.1. Data for compounds

3.1.1. Diamine 8b. A 500-mL, three-necked, round-bottomed flask, equipped with a nitrogen inlet adapter, a glass stopper, a gas inlet adapter fitted with a hydrogen balloon, and a magnetic stirring bar was charged with 250 mL of methanol, potassium acetate (8.80 g, 89.7 mmol), Boc-glycinal[27] (8.28 g, 28.2 mmol), *N*-phenylpropylenediamine[17] (6.70 g, 44.6 mmol), and 7.61 g of 10% Pd/C. The flask was evacuated and filled with nitrogen

twice, and then evacuated, filled with hydrogen, and maintained under a hydrogen atmosphere for 13 h. The reaction mixture was filtered and concentrated by rotary evaporation. The residue was dissolved in 150 mL of 1.0 M NaOH and the solution was extracted with three 100-mL portions of methylene chloride. The combined organic layers were dried over Na_2SO_4 and concentrated by rotary evaporation to 13.77 g of a yellow oil. The crude product was purified by column chromatography on silica gel (EtOAc–*i*-PrOH, 1:1) to afford 3.05 g of **8b** as a pale yellow oil (23%): IR (neat) 3365, 1697 cm^{-1}; ^1H NMR (500 MHz, $CDCl_3$) δ 7.15 (dd, J=8.5, 7.3 Hz, 2H), 6.67 (tt, J=7.3, 1.0 Hz, 1H), 6.59 (dd, J=8.6, 1.0 Hz, 2H), 5.06 (br. s, 1H), 3.20 (br. q, J=5.6 Hz, 2H), 3.16 (t, J=6.6 Hz, 2H), 2.71 (t, J=6.7 Hz, 2H), 2.70 (t, J=5.9 Hz, 2H), 1.76 (quintet, J=6.6 Hz, 2H), 1.44 (s, 9H); ^{13}C NMR (125 MHz, $CDCl_3$) δ 156.0, 148.4, 129.0, 116.9, 112.5, 79.0, 49.1, 47.6, 42.4, 40.1, 29.3, 28.3; HRMS *m/e* calcd for $C_{16}H_{28}N_3O_2$ $(M+H)^+$, 294.2181 found: 294.2181; Anal. Calcd for $C_{16}H_{27}N_3O_2$: C, 65.50; H, 9.28; N, 14.32. Found: C, 65.16; H, 9.04; N, 14.08.

3.1.2. Diurea 9a. A solution of diamine **8a**[13] (0.178 g, 0.637 mmol) and 0.224 g of valylalanine methyl ester isocyanate (70% purity by ^1H NMR analysis, 0.69 mmol) in 30 mL of methylene chloride was stirred under nitrogen for 1 h and then concentrated by rotary evaporation. The residue was purified by column chromatography on silica gel (EtOAc–hexanes, 2:1) to afford 0.319 g (99%) of $PhNHCH_2CH_2N(CO–Val–Ala–OMe)CH_2CH_2NHBoc$ as a white foam.

A mixture of $PhNHCH_2CH_2N(CO–Val–Ala–OMe)$-$CH_2CH_2NHBoc$ (0.296 g, 0.583 mmol) and phenylalanylleucine methyl ester isocyanate[20] (0.225 g, 0.710 mmol) in 13 mL of 1,2-dichloroethane was heated at reflux under nitrogen for 36 h and then concentrated by rotary evaporation. Radial thin-layer chromatography on silica gel (sequential elution with EtOAc–hexanes, 3:2, EtOAc–hexanes, 2:1, and EtOAc–*i*-PrOH, 95:5) afforded 0.359 g (75%) of diurea **9a** as a sticky white foam: IR ($CHCl_3$) 3419, 3338, 1741, 1697, 1674, 1645 cm^{-1}; ^1H NMR (500 MHz, $CDCl_3$) δ 7.38–7.35 (m, 2H), 7.34–7.30 (m, 1H), 7.25–7.23 (m, 3H), 7.10–7.08 (m, 2H), 7.01–6.99 (m, 2H), 6.96 (d, J=7.0 Hz, 1H), 6.77 (br s, 1H), 6.45 (br s, 1H), 5.23 (br t, J=4.3 Hz, 1H), 4.76 (d, J=7.7 Hz, 1H), 4.61 (q, J=7.2 Hz, 1H), 4.57 (q, J=7.3 Hz, 1H), 4.48 (td, J=8.3, 5.3 Hz, 1H), 4.15 (t, J=7.4 Hz, 1H), 3.78–3.71 (m, 1H), 3.71 (s, 3H), 3.70 (s, 3H), 3.62–3.55 (m, 1H), 3.49–3.36 (m, 3H), 3.31–3.20 (m, 2H), 3.19–3.12 (m, 1H), 3.02 (dd, ABX pattern J_{AB}=13.9 Hz, J_{AX}=6.7 Hz, 1H), 2.96 (dd ABX pattern, J_{AB}=14.0 Hz, J_{BX}=7.4 Hz, 1H), 2.29 (octet, J=6.7 Hz, 1H), 1.61–1.54 (m, 1H), 1.52–1.45 (m, 2H), 1.388 (s, 9H), 1.385 (d, J=6.8 Hz, 3H), 1.04 (d, J=6.8 Hz, 3H), 1.02 (d, J=6.8 Hz, 3H), 0.88 (d, J=6.2 Hz, 3H), 0.86 (d, J=6.2 Hz, 3H); ^{13}C NMR (125 MHz, $CDCl_3$) δ 173.5, 172.9, 172.2, 171.2, 158.0, 156.6, 156.3, 141.1, 136.7, 130.2, 129.2, 128.4, 128.3, 128.0, 127.5, 126.7, 79.0, 60.8, 55.1, 52.0, 50.7, 48.9, 47.6, 47.3, 46.2, 40.8, 39.7, 37.8, 30.4, 28.2, 24.7, 22.6, 21.7, 19.4, 18.6, 18.1; HRMS (FAB) *m/e* for $C_{42}H_{64}N_7O_{10}$ $(M+H)^+$, calcd 826.4714, found: 826.4717; Anal. Calcd for $C_{42}H_{63}N_7O_{10}$: C, 61.07; H, 7.69; N, 11.87. Found: C, 61.19; H, 7.72; N, 11.77.

3.1.3. Diurea 9b. Diamine **8b** was converted to diurea **9b** in 84% yield, as described earlier: IR ($CHCl_3$) 3421, 3338, 1741, 1672, 1645 cm^{-1}; ^1H NMR (500 MHz, $CDCl_3$) δ 7.36 (appar t, J=7.2 Hz, 2H), 7.31 (appar t, J=7.3 Hz, 1H), 7.23–7.19 (m, 3H), 7.04–7.01 (m, 4H), 6.93 (d, J=6.9 Hz, 1H), 6.83 (d, J=7.8 Hz, 1H), 5.93 (d, J=7.9 Hz, 1H), 5.30 (appar t, J=5.0 Hz, 1H), 4.60–4.52 (m, 3H), 4.49 (td, J=8.2, 5.3 Hz, 1H), 4.18 (t, J=7.4 Hz, 1H), 3.71 (s, 3H), 3.70 (s, 3H), 3.69–3.58 (m, 2H), 3.35–3.17 (m, 6H), 2.99 (dd ABX pattern, J_{AB}=14.0 Hz, J_{AX}=5.6 Hz, 1H), 2.91 (dd ABX pattern, J_{AB}=14.0 Hz, J_{BX}=6.9 Hz, 1H), 2.21–2.15 (m, 1H), 1.78–1.65 (m, 2H), 1.62–1.45 (m, 3H), 1.41 (s, 9H), 1.37 (d, J=7.2 Hz, 3H), 0.95 (appar t, J=7.5 Hz, 6H), 0.89 (d, J=6.2 Hz, 3H), 0.87 (d, J=6.2 Hz, 3H); ^{13}C NMR (125 MHz, $CDCl_3$) δ 173.2, 173.0, 172.2, 171.5, 157.6, 156.3, 140.5, 136.6, 130.0, 129.1, 128.2, 128.1, 127.8, 126.4, 79.1, 59.8, 54.9, 52.0, 50.6, 47.6, 46.7, 46.3, 45.1, 40.7, 39.4, 37.6, 30.7, 28.1, 27.4, 24.5, 22.5, 21.7, 19.2, 18.2, 17.6; HRMS (FAB) *m/e* for $C_{43}H_{66}N_7O_{10}$ $(M+H)^+$, calcd 840.4871 found: 840.4882; Anal. Calcd for $C_{43}H_{65}N_7O_{10}$: C, 61.48; H, 7.80; N, 11.67. Found: C, 61.34; H, 7.90; N, 11.47.

3.1.4. Secondary amine 10a. A solution of diurea **9a** (0.317 g, 0.383 mmol) in 15 mL of methylene chloride and 1.2 mL of trifluoroacetic acid was stirred for 90 min and then concentrated by rotary evaporation. The residue was partitioned between 20 mL of methylene chloride and 20 mL of saturated aqueous sodium bicarbonate. The aqueous layer was extracted with two 20-mL portions of methylene chloride, and the combined organic layers were dried over Na_2SO_4 and concentrated by rotary evaporation to afford 0.278 g (100%) of $PhN(CO–Phe–Leu–OMe)$-$CH_2CH_2N(CO–Val–Ala–OMe)CH_2CH_2NH_2$ as a colorless oil.

A solution of $PhN(CO–Phe–Leu–OMe)CH_2CH_2N(CO–Val–Ala–OMe)CH_2CH_2NH_2$ (0.278 g, 0.383 mmol) in 20 mL of methanol and 0.5 mL acrylonitrile (0.4 g, 8 mmol) was stirred under nitrogen for 7 h and then concentrated by rotary evaporation. Column chromatography on silica gel (EtOAc–*i*-PrOH, 9:1) afforded 0.249 g (84%) of secondary amine **10a** as a white foam: IR ($CHCl_3$) 3419, 3325, 2251, 1741, 1672, 1643 cm^{-1}; ^1H NMR (500 MHz, $CDCl_3$) δ 7.36 (t, J=7.4 Hz, 2H), 7.32–7.29 (m, 1H), 7.25–7.19 (m, 3H), 7.08–7.06 (m, 2H), 7.04 (d, J=7.7 Hz, 2H), 6.88 (br d, J=5.8 Hz, 1H), 6.80 (d, J=8.4 Hz, 1H), 6.65 (br s, 1H), 4.75 (d, J=7.4 Hz, 1H), 4.59–4.52 (m, 2H), 4.48 (td, J=8.0, 5.5 Hz, 1H), 4.09 (t, J=7.5 Hz, 1H), 3.78–3.63 (m, 2H), 3.71 (s, 3H), 3.70 (s, 3H), 3.50–3.44 (m, 1H), 3.43–3.35 (m, 2H), 3.33–3.28 (m, 1H), 3.01 (dd ABX pattern, J_{AB}=13.9 Hz, J_{AX}=6.4 Hz, 1H), 2.95 (dd ABX pattern, J_{AB}=14.0 Hz, J_{BX}=7.5 Hz, 1H), 2.93–2.87 (m, 2H), 2.80–2.72 (m, 2H), 2.56–2.45 (m, 2H), 2.16 (sextet, J=6.7 Hz, 1H), 1.68 (br s, 1H), 1.61–1.55 (m, 1H), 1.54–1.46 (m, 2H), 1.36 (d, J=7.2 Hz, 3H), 0.98 (d, J= 6.7 Hz, 6H), 0.89 (d, J=6.2 Hz, 3H) 0.86 (d, J=6.2 Hz, 3H); ^{13}C NMR (125 MHz, $CDCl_3$) δ 173.4, 173.0, 172.2, 171.2, 158.6, 156.6, 141.3, 136.8, 130.2, 129.3, 128.4, 128.0, 127.7, 126.7, 118.7, 60.5, 55.2, 52.20, 52.17, 50.8, 48.8, 48.4, 47.8, 46.4, 45.2, 41.0, 37.7, 30.7, 24.7, 22.7, 21.8, 19.4, 18.5, 18.1; HRMS (FAB) *m/e* for $C_{40}H_{59}N_8O_8$ $(M+H)^+$, calcd 779.4455, found: 779.4456; Anal. Calcd for

$C_{40}H_{58}N_8O_9$: C, 61.68; H, 7.51; N, 14.39. Found: C, 61.68; H, 7.87; N, 14.02.

3.1.5. Secondary amine 10b. Diurea **9b** was converted to secondary amine **10b** in 82% yield, as described earlier: IR ($CHCl_3$) 3423, 3294, 2251, 1741, 1670, 1645 cm^{-1}; ^1H NMR (500 MHz, $CDCl_3$) δ 7.36 (appar t, 7.1 Hz, 2H), 7.31 (appar t, J=7.3 Hz, 1H), 7.23–7.19 (m, 3H), 7.05–7.01 (m, 4H), 6.85 (d, J=7.7 Hz, 1H), 6.65 (d, J= 7.2 Hz, 1H), 6.64 (br s, 1H), 4.57 (td, J=7.6, 6.3 Hz, 1H), 4.52–4.45 (m, 3H), 4.07 (dd, J=8.5, 6.6 Hz, 1H), 3.73 (s, 3H), 3.71 (s, 3H), 3.71–3.66 (m, 1H), 3.60–3.55 (m, 1H), 3.47–3.34 (m, 2H), 3.25–3.19 (m, 2H), 3.00–2.89 (m, 4H), 2.86–2.76 (m, 2H), 2.63 (dt, J=16.8, 6.9 Hz, 1H), 2.55 (dt, J=16.9, 6.7 Hz, 1H), 2.08 (octet, J=6.7 Hz, 1H), 1.84 (br s, 1H), 1.69 (quintet, J=7.1 Hz, 2H), 1.62–1.50 (m, 3H), 1.37 (d, J= 7.2 Hz, 3H), 0.95 (d, J=6.8 Hz, 3H), 0.93 (d, J=6.8 Hz, 3H), 0.90 (d, J=6.0 Hz, 3H), 0.87 (d, J=6.0 Hz, 3H); ^{13}C NMR (125 MHz, $CDCl_3$) δ 173.0, 172.9, 172.3, 171.6, 158.7, 156.0, 140.4, 136.6, 129.8, 129.0, 128.00, 127.97, 127.6, 126.2, 118.6, 59.4, 54.6, 51.8, 50.5, 48.3, 47.6, 46.5, 45.2, 44.9, 40.5, 37.5, 30.8, 27.1, 24.4, 22.4, 21.5, 19.0, 18.1, 18.0, 17.2; HRMS (FAB) *m/e* for $C_{41}H_{61}N_8O_8$ $(M+H)^+$, calcd 793.4612, found: 793.4635; Anal. Calcd for $C_{41}H_{60}N_8O_8$: C, 62.10; H, 7.63; N, 14.13. Found: C, 61.99; H, 7.83; N, 13.89.

3.1.6. Diamide 11a. A solution of secondary amine **10a** (0.224 g, 0.288 mmol) in 20 mL of a 47% (w/w) solution of methylamine in methanol was stirred for 45 min and then concentrated by rotary evaporation to afford 0.227 g (101%) of diamide **11a** as a sticky white foam: IR ($CHCl_3$) 3417, 3338, 2251, 1659 cm^{-1}; ^1H NMR (500 MHz, $CDCl_3$) δ 7.37–7.27 (m, 4H), 7.20–7.17 (m, 4H), 7.09 (br s, 1H), 7.03 (d, J=7.0 Hz, 2H), 6.98–6.97 (m, 2H), 6.79 (d, J= 6.5 Hz, 1H), 6.76 (br s, 1H), 6.69 (d, J=6.0 Hz, 1H), 4.56–4.52 (m, 1H), 4.50 (quintet, J=7.2 Hz, 1H), 4.40 (td, J=8.9, 4.7 Hz, 1H), 4.08 (t, J=6.7 Hz, 1H), 3.83–3.79 (m, 1H), 3.70–3.65 (m, 1H), 3.59–3.53 (m, 1H), 3.36–3.27 (m, 2H), 3.22–3.17 (m, 1H), 3.02 (dd ABX pattern, J_{AB}= 13.7 Hz, J_{AX}=6.2 Hz, 1H), 2.94 (dd ABX pattern, J_{AB}= 13.8 Hz, J_{BX}=7.3 Hz, 1H), 2.88 (t, J=6.5 Hz, 2H), 2.79–2.69 (m, 2H), 2.71 (d, J=5.1 Hz, 3H), 2.70 (d, J=5.4 Hz, 3H), 2.53–2.46 (m, 2H), 2.15 (octet, J=6.6 Hz, 1H), 1.72 (ddd, J=13.9, 9.0, 5.0 Hz, 1H), 1.62–1.55 (m, 1H), 1.52–1.44 (m, 1H), 1.36 (d, J=7.0 Hz, 3H), 0.97 (appar t, J= 5.9 Hz, 6H), 0.89 (d, J=6.6 Hz, 3H), 0.86 (d, J=6.5 Hz, 3H); ^{13}C NMR (125 MHz, $CDCl_3$) δ 172.9, 172.5, 172.3, 171.7, 158.7, 156.8, 141.4, 136.3, 130.1, 129.0, 128.4, 128.0, 127.5, 126.7, 118.6, 60.8, 55.6, 51.8, 48.8, 48.6, 48.2, 48.0, 45.9, 45.1, 40.0, 37.4, 30.6, 26.1, 26.0, 24.6, 23.0, 21.6, 19.4, 18.4, 18.3, 18.1; HRMS (FAB) *m/e* for $C_{40}H_{61}N_{10}O_6$ $(M+H)^+$, calcd 777.4775, found: 777.4773; Anal. Calcd for $C_{40}H_{60}N_{10}O_6$: C, 61.83; H, 7.78; N, 18.03. Found: C, 62.14; H, 7.97; N, 18.14.

3.1.7. Diamide 11b. Secondary amine **10b** was converted to diamide **11b** in 98% yield as described earlier: IR ($CHCl_3$) 3415, 3325, 2251, 1657 cm^{-1}; ^1H NMR (500 MHz, $CDCl_3$) δ 7.39–7.33 (m, 3H), 7.22–7.15 (m, 3H), 7.07–7.04 (m, 3H), 6.94–6.92 (m, 2H), 6.91 (d, J=8.7 Hz, 1H), 6.81 (br q, J=4.7 Hz, 1H), 6.68 (br q, J=4.5 Hz, 1H), 6.63 (br s, 1H), 4.55 (d, J=6.5 Hz, 1H), 4.50–4.38 (m, 3H), 4.03 (dd, J=7.3, 6.5 Hz, 1H), 3.79–3.74 (m, 1H), 3.49–3.38 (m, 3H), 3.29–3.16 (m, 2H), 3.01 (dd ABX pattern, J_{AB}=13.8 Hz, J_{AX}= 6.1 Hz, 1H), 2.94 (td, J=6.6, 1.3 Hz, 2H), 2.88–2.77 (m, 3H), 2.73 (d, J=4.8 Hz, 3H), 2.70 (d, J=4.8 Hz, 3H), 2.60 (dt, J=16.8, 6.7 Hz, 1H), 2.55 (dt, J=16.8, 6.5 Hz, 1H), 2.14 (octet, J=6.7 Hz, 1H), 1.86–1.65 (m, 4H), 1.59–1.45 (m, 2H), 1.37 (d, J=7.1 Hz, 3H), 0.95 (appar t, J=6.4 Hz, 6H), 0.90 (d, J=6.6 Hz, 3H), 0.87 (d, J=6.5 Hz, 3H); ^{13}C NMR (125 MHz, $CDCl_3$) δ 172.8, 172.6, 172.5, 171.8, 159.0, 156.7, 140.5, 136.2, 130.2, 128.9, 128.5, 128.1, 126.7, 118.7, 60.4, 55.8, 51.6, 48.8, 48.6, 48.4, 46.9, 45.3, 45.2, 40.1, 37.4, 30.7, 27.5, 26.2, 26.1, 24.7, 23.1, 21.5, 19.4, 18.3, 17.6; HRMS (FAB) *m/e* for $C_{41}H_{63}N_{10}O_6$ $(M+H)^+$, calcd 791.4932, found: 791.4927; Anal. Calcd for $C_{41}H_{62}N_{10}O_6$: C, 62.26; H, 7.90; N, 17.71. Found: C, 62.18; H, 8.08; N, 17.43.

3.1.8. Artificial β-sheet 5a. A solution of diamide **11a** (0.104 g, 0.134 mmol) and isocyanate **12**[15a] (0.030 g, 0.145 mmol) in 15 mL of methylene chloride was stirred under nitrogen for 6 h and then concentrated by rotary evaporation. Radial thin-layer chromatography on silica gel (EtOAc–*i*-PrOH, 9:1) followed by preparative reverse-phase HPLC (C_{18} column, 40:60 acetonitrile–water eluant) afforded 0.118 g (90%) of artificial β-sheet **5a** as a glassy white solid: IR ($CHCl_3$) 3410, 3294, 2251, 1657, 1645 cm^{-1}; ^1H NMR (500 MHz, $CDCl_3$) δ 9.92 (br s, 1H), 8.422 (d, J=1.5 Hz, 1H), 8.418 (br s, 1H), 8.26 (dd, J=8.8, 1.8 Hz, 1H), 8.15 (br q, J=4.7 Hz, 1H), 7.37–7.29 (m, 4H), 7.20–7.17 (m, 3H), 7.05–6.99 (m, 5H), 6.89 (d, J=9.1 Hz, 1H), 6.73–6.61 (m, 2H), 4.70 (d, J=6.9 Hz, 1H), 4.59 (q, J=6.7 Hz, 1H), 4.44–4.34 (m, 2H), 4.11 (t, J= 8.3 Hz, 1H), 3.93 (s, 3H), 3.78–3.67 (m, 2H), 3.60–3.52 (m, 2H), 3.47–3.41 (m, 1H), 3.37–3.24 (m, 5H), 3.05 (dd, ABX pattern, J_{AB}=13.8 Hz, J_{AX}=6.1 Hz, 1H), 3.00 (d, J= 4.7 Hz, 3H), 2.95 (dd, ABX pattern, J_{AB}=13.7 Hz, J_{BX}= 7.2 Hz, 1H), 2.70 (d, J=5.0 Hz, 3H), 2.69 (d, J=5.0 Hz, 3H), 2.69–2.63 (m, 1H), 2.58 (dt, J=16.9, 6.1 Hz, 1H), 2.16–2.08 (m, 1H), 1.66 (ddd, J=13.9, 8.6, 5.4 Hz, 1H), 1.53 (ddd, J=14.5, 9.7, 5.6 Hz), 1.46–1.38, (m, 1H), 1.22 (d, J=7.0 Hz, 3H), 1.08 (d, J=6.5 Hz, 3H), 1.04 (d, J=6.6 Hz, 3H), 0.84 (d, J=6.6 Hz, 3H), 0.81 (d, J= 6.5 Hz, 3H); ^{13}C NMR (125 MHz, $CDCl_3$) δ 173.0, 172.7, 172.4, 171.5, 166.0, 159.0, 157.4, 155.4, 152.5, 141.3, 136.3, 134.4, 130.2, 129.0, 128.4, 128.1, 127.4, 126.7, 122.6, 122.1, 120.5, 118.8, 111.6, 62.1, 56.0, 55.8, 51.8, 49.7, 49.1, 48.5, 47.6, 47.3, 45.2, 39.8, 37.6, 30.0, 26.4, 26.1, 25.9, 24.6, 22.8, 21.6, 19.5, 19.3, 17.5, 16.8; HRMS (FAB) *m/e* calcd for $C_{50}H_{71}N_{12}O_9$ $(M+H)^+$, 983.5467 found: 983.5472; Anal. Calcd for $C_{50}H_{70}N_{12}O_9$: C, 61.08; H, 7.18; N, 17.10. Found: C, 61.43; H, 7.10; N, 17.07.

3.1.9. Artificial β-sheet 5b. Diamide **11b** was converted to artificial β-sheet **5b** in 93% yield by treatment with isocyanate **12**,[15a] as described earlier: IR ($CHCl_3$) 3410, 3294, 2251, 1659 cm^{-1}; ^1H NMR (500 MHz, $CDCl_3$) δ 10.05 (br s, 1H), 8.43 (br s, 1H), 8.42 (d, J=2.4 Hz, 1H), 8.32 (dd, J=8.9, 2.4 Hz, 1H), 8.14 (q, J=4.8 Hz, 1H), 7.41 (appar t, J=7.1 Hz, 2H), 7.37 (appar t, J=7.2 Hz, 1H), 7.22–7.20 (m, 3H), 7.13 (br d, J=7.8 Hz, 1H), 7.06–7.04 (m, 2H), 7.01–6.99 (m, 2H), 6.91 (br s, 1H), 6.90 (d, J= 9.1 Hz, 1H), 6.39 (br s, 1H), 6.34 (br s, 1H), 4.68 (d, J= 7.0 Hz, 1H), 4.63 (q, J=7.0 Hz, 1H), 4.42–4.38 (m, 1H),

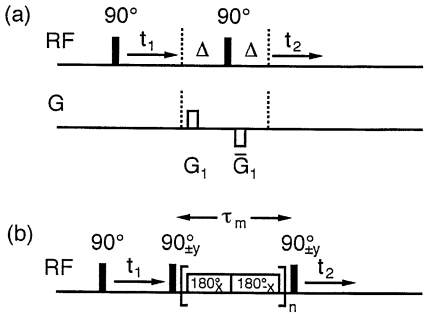

Figure 4. Pulse sequences used in this work. (a) PFG COSY with P-type selection. A fixed delay Δ=25 ms was used to allow the spectra to be recorded with fewer t_1 increments. The PFGs were 3 G cm^{-1} in strength and 1 ms in duration. Connectivities can be quickly determined but coupling constants cannot be measured. (b) Tr-ROESY pulse sequence. The 90°($\pm y$) purging pulses allow a phase-sensitive two-dimensional spectrum to be obtained. Throughout the mixing period a train of phase alternating 180° pulses spin locks y-magnetization while inhibiting TOCSY transfer. The RF field strength was 6 kHz during τ_m. As in conventional ROESY, weak spurious COSY-type cross peaks can arise from zero-quantum coherence.

4.31 (quintet, *J*=7.1 Hz, 1H), 4.16 (t, *J*=8.5 Hz, 1H), 3.94 (s, 3H), 3.83 (dt, *J*=14.2, 6.2 Hz, 1H), 3.58 (t, *J*=6.3 Hz, 2H), 3.55–3.51 (m, 2H), 3.46–3.38 (m, 3H), 3.33 (dt, *J*=15.4, 6.8 Hz, 1H), 3.24 (dt, *J*=15.3, 6.7 Hz, 1H), 3.01 (d, *J*=4.8 Hz, 3H), 3.01–2.97 (m, 1H), 2.86 (dd ABX pattern, J_{AB}=13.8 Hz, J_{AX}=7.3 Hz, 1H), 2.69 (t, *J*=6.3 Hz, 2H), 2.67 (d, *J*=4.8 Hz, 6H), 2.22–2.14 (m, 1H), 1.87–1.78 (m, 1H), 1.73–1.65 (m, 2H), 1.55–1.46 (m, 2H), 1.22 (d, *J*=7.1 Hz, 3H), 1.05 (d, *J*=6.6 Hz, 3H), 1.04 (d, *J*=6.5 Hz, 3H), 0.99 (d, *J*=6.4 Hz, 3H), 0.97 (d, *J*=6.4 Hz, 3H); ^{13}C NMR (125 MHz, $CDCl_3$) δ 173.4, 172.8, 172.3, 171.6, 166.0, 158.8, 156.5, 155.4, 152.3, 140.2, 136.3, 134.5, 130.2, 129.0, 128.3, 128.1, 126.6, 122.4, 121.9, 120.3, 118.9, 111.6, 62.4, 56.0, 55.5, 51.4, 49.4, 48.4, 48.0, 46.5, 45.6, 45.0, 40.4, 37.9, 29.7, 28.0, 26.4, 26.0, 25.7, 24.6, 22.8, 21.6, 19.6, 19.4, 17.5, 16.6; HRMS (FAB) *m/e* calcd for $C_{51}H_{73}N_{12}O_9$ $(M+H)^+$, 997.5623 found: 997.5632; Anal. Calcd for $C_{51}H_{72}N_{12}O_9$: C, 61.43; H, 7.28; N, 16.85. Found: C, 61.66; H, 7.47; N, 16.72.

3.1.10. Artificial β-sheet 6a. Diamide **11a** was converted to artificial β-sheet **6a** in 88% yield by treatment with isocyanate **13**,[15a] as described earlier: IR ($CHCl_3$) 3423, 3304, 2249, 1655, 1630 cm^{-1}; ^{1}H NMR (500 MHz, $CDCl_3$) δ 11.03 (br d, *J*=5.3 Hz, 1H), 10.86 (d, *J*=7.1 Hz, 1H), 10.01 (s, 1H), 8.58 (d, *J*=2.6 Hz, 1H), 8.52 (d, *J*=9.2 Hz, 1H), 8.34 (dd, *J*=9.0, 2.8 Hz, 1H), 8.09 (d, *J*=8.6 Hz, 1H), 7.85 (br q, *J*=4.3 Hz, 1H), 7.30 (appar t, *J*=7.6 Hz, 2H), 7.25 (appar t, *J*=7.4 Hz, 1H), 7.20–7.16 (m, 3H), 7.09 (d, *J*=7.5 Hz, 2H), 7.05–7.04 (m, 2H), 6.90 (d, *J*=9.1 Hz, 1H), 6.72 (br q, *J*=3.4 Hz, 1H), 6.25 (d, *J*=8.5 Hz, 1H), 4.78 (ddd, *J*=8.4, 6.9, 5.5 Hz, 1H), 4.68 (dq, *J*=8.1, 6.9 Hz, 1H), 4.42 (d, *J*=8.7 Hz, 1H), 4.32–4.27 (m, 2H), 4.18 (ddd, *J*=15.5, 11.1, 4.9 Hz, 1H), 4.01 (s, 3H), 3.98 (dd, *J*=14.3, 4.2 Hz, 1H), 3.46 (br t, *J*=6.0 Hz, 2H), 3.40 (ddd, *J*=14.3, 11.2, 5.3 Hz, 1H), 3.26 (br s, 2H), 3.16 (dd ABX pattern, J_{AB}=13.4 Hz, J_{AX}=5.1 Hz, 1H), 3.15 (br s, 2H), 3.09 (dd, *J*=15.6, 4.5 Hz, 1H), 3.03 (dd ABX pattern, J_{AB}=13.5 Hz, J_{BX}=7.0 Hz, 1H), 2.88 (septet, *J*=6.9 Hz, 1H), 2.81 (d, *J*=4.6 Hz, 3H), 2.70 (d, *J*=4.8 Hz, 3H), 2.63 (dt, *J*=17.0, 6.3 Hz, 1H), 2.54 (dt, *J*=17.0, 6.1 Hz, 1H), 1.99 (octet, *J*=6.9 Hz, 1H), 1.74 (ddd, *J*=14.1, 8.5, 5.7 Hz, 1H), 1.65 (ddd, *J*=14.5, 9.5, 5.7 Hz, 1H), 1.27 (d, *J*=6.9 Hz, 3H), 1.24 (d, *J*=6.9 Hz, 3H), 1.23–1.17 (m, 1H), 1.12 (d, *J*=6.8 Hz, 3H), 1.03 (d, *J*=6.7 Hz, 3H), 0.95 (d, *J*=6.7 Hz, 3H), 0.78 (d, *J*=6.7 Hz, 3H), 0.72 (d, *J*=6.6 Hz, 3H); ^{13}C NMR (125 MHz, $CDCl_3$) δ 173.1, 173.0, 172.2, 172.0, 159.8, 159.2, 158.1, 155.3, 152.2, 142.1, 136.7, 134.7, 130.1, 129.5, 128.2, 127.8, 127.3, 126.5, 122.8, 121.6, 118.8, 111.4, 61.0, 56.2, 55.4, 51.7, 50.4, 47.9, 47.5, 47.3, 46.9, 45.1, 38.7, 37.1, 32.8, 31.2, 25.93, 25.87, 24.4, 22.9, 21.5, 19.5, 19.3, 19.1, 18.0, 17.5; HRMS (FAB) *m/e* calcd for $C_{53}H_{76}N_{13}O_{10}$ $(M+H)^+$, 1054.5838 found: 1054.5835; Anal. Calcd for $C_{53}H_{75}N_{13}O_{10}$: C, 60.38; H, 7.17; N, 17.27. Found: C, 60.58; H, 7.38; N, 17.13.

3.1.11. Artificial β-sheet 6b. Diamide **11b** was converted to artificial β-sheet **6b** in 98% yield by treatment with isocyanate **13**,[15a] as described above: IR ($CHCl_3$) 3423, 3304, 2249, 1655, 1630 cm^{-1}; ^{1}H NMR (500 MHz, $CDCl_3$) δ 11.18 (d, *J*=6.5 Hz, 1H), 11.02 (d, *J*=7.8 Hz, 1H), 10.41 (s, 1H), 8.78 (d, *J*=9.3 Hz, 1H), 8.72 (s, 1H), 8.36 (dd, *J*=9.0, 2.8 Hz, 1H), 8.18 (d, *J*=8.9 Hz, 1H), 7.41 (appar t, *J*=7.5 Hz, 2H), 7.35 (appar t, *J*=7.4 Hz, 1H), 7.32 (br q, *J*=4.4 Hz, 1H), 7.23–7.17 (m, 3H), 7.12 (appar dd, *J*=7.4, 1.7 Hz, 2H), 7.07 (appar d, *J*=7.5 Hz, 2H), 6.94 (d, *J*=9.0 Hz, 1H), 6.91 (d, *J*=9.1 Hz, 1H), 5.94 (br s, 1H), 4.95 (td, *J*=8.4, 6.4 Hz, 1H), 4.75 (d, *J*=8.3 Hz, 1H), 4.67 (dq, *J*=9.3, 7.1 Hz, 1H), 4.49 (t, *J*=9.0 Hz, 1H), 4.37 (td, *J*=9.1, 5.8 Hz, 1H), 4.02 (s, 3H), 3.81 (dt, *J*=14.0, 4.6 Hz, 1H), 3.65–3.60 (m, 2H), 3.58–3.52 (m, 3H), 3.47–3.43 (m, 1H), 3.42–3.37 (m, 2H), 3.26 (appar dt, *J*=15.2, 7.6 Hz, 1H), 2.99 (dd ABX pattern, J_{AB}=13.5 Hz, J_{AX}=9.0 Hz, 1H), 2.96–2.89 (m, 2H), 2.79 (d, *J*=4.6 Hz, 3H), 2.71 (dt, *J*=17.0, 6.2 Hz, 1H), 2.67 (dt, *J*=17.0, 6.2 Hz, 1H), 2.59 (d, *J*=4.7 Hz, 3H), 2.29–2.20 (m, 1H), 2.11–2.02 (m, 1H), 1.73–1.66 (m, 2H), 1.59 (ddd, *J*=13.8, 9.4, 5.8 Hz, 1H), 1.54–1.44 (m, 1H), 1.26 (d, *J*=6.8 Hz, 3H), 1.21 (d, *J*=6.9 Hz, 6H), 1.09 (d, *J*=6.6 Hz, 3H), 0.97 (d, *J*=6.7 Hz, 3H), 0.88 (d, *J*=6.7 Hz, 3H), 0.84 (d, *J*=6.6 Hz, 3H); ^{13}C NMR (125 MHz, $CDCl_3$) δ 173.2, 172.50, 172.47, 172.1, 171.3, 159.1, 158.8, 156.8, 155.5, 152.1, 141.1, 136.8, 134.8, 130.2, 129.1, 128.11, 128.05, 127.7, 126.3, 122.8, 121.7, 119.0, 118.5, 111.3, 61.3, 56.1, 55.6, 50.9, 48.5, 48.2, 47.7, 47.5, 46.5, 45.3, 39.8, 38.2, 32.4, 31.3, 28.8, 25.9, 25.8, 24.7, 22.7, 22.0, 19.5, 19.4, 19.3, 19.2, 17.9, 17.6; HRMS (FAB) *m/e* calcd for $C_{54}H_{78}N_{13}O_{10}$ $(M+H)^+$, 1068.5994 found: 1068.5986; Anal. Calcd for $C_{54}H_{77}N_{13}O_{10}$: C, 60.71; H, 7.27; N, 17.04. Found: C, 60.65; H, 6.97; N, 16.91.

3.2. Two-dimensional ^{1}H NMR spectroscopic studies of artificial β-sheets 6a and 6b

Studies were performed at 500 MHz using a 25 mM sample in $CDCl_3$ that was degassed by five freeze-pump-thaw cycles on a high-vacuum line (<0.001 mmHg) and sealed under vacuum. Two-dimensional ^{1}H NMR spectra were recorded at 298 K, as were one-dimensional reference spectra. Magnitude-mode COSY spectra were obtained using P-type selection with bipolar pulsed field gradients (PFGs) bracketing the mixing pulse, as shown in Fig. 4a.[28] A fixed delay Δ in both t_1 and t_2 served to improve

Table 2. ^{1}H NMR spectral data for artificial β-sheets **6**

Resonance	Artificial β-sheet **6a**	Artificial β-sheet **6b**
1	0.72 (d, *J*=6.6 Hz, 3H)	0.84 (d, *J*=6.6 Hz, 3H)
2	0.78 (d, *J*=6.7 Hz, 3H)	0.88 (d, *J*=6.7 Hz, 3H)
3	0.95 (d, *J*=6.7 Hz, 3H)	0.97 (d, *J*=6.7 Hz, 3H)
4	1.03 (d, *J*=6.7 Hz, 3H)	1.09 (d, *J*=6.6 Hz, 3H)
5	1.12 (d, *J*=6.8 Hz, 3H)	1.21 (d, *J*=6.9 Hz, 6H)
6	1.23–1.17 (m, 1H)	1.26 (d, *J*=6.8 Hz, 3H)
7	1.24 (d, *J*=6.9 Hz, 3H)	1.54–1.44 (m, 1H)
8	1.27 (d, *J*=6.9 Hz, 3H)	1.59 (ddd, *J*=13.8, 9.4, 5.8 Hz, 1H)
9	1.65 (ddd, *J*=13.9, 9.5, 5.7 Hz, 1H)	1.73–1.66 (m, 2H)
10	1.74 (ddd, *J*=13.9, 8.5, 5.7 Hz, 1H)	2.11–2.02 (m, 1H)
11	1.99 (octet, *J*=6.9 Hz, 1H)	2.29–2.20 (m, 1H)
12	2.54 (dt, *J*=17.0, 6.1 Hz, 1H)	2.59 (d, *J*=4.7 Hz, 3H)
13	2.63 (dt, *J*=17.0, 6.3 Hz, 1H)	2.67 (dt, *J*=17.0, 6.2 Hz, 1H)
14	2.70 (d, *J*=4.8 Hz, 3H)	2.71 (dt, *J*=17.0, 6.2 Hz, 1H)
15	2.81 (d, *J*=4.6 Hz, 3H)	2.79 (d, *J*=4.6 Hz, 3H)
16	2.88 (septet, *J*=6.9 Hz, 1H)	2.96–2.89 (m, 2H)
17	3.03 (dd ABX pattern, J_{AB}=13.5 Hz, J_{AX}=7.0 Hz, 1H)	2.99 (dd ABX pattern, J_{AB}=13.5 Hz, J_{AX}=9.0 Hz, 1H)
18	3.09 (dd, *J*=15.6, 4.5 Hz, 1H)	3.26 (appar dt, *J*=15.2, 7.6 Hz, 1H)
19	3.15 (br s, 2H)	3.42–3.37 (m, 2H)
19′	3.16 (dd ABX pattern, J_{AB}=13.4 Hz, J_{BX}=5.1 Hz, 1H)	
20	3.26 (br s, 2H)	3.47–3.43 (m, 1H)
21	3.40 (ddd, *J*=14.3, 11.2, 5.3 Hz, 1H)	3.58–3.52 (m, 3H)
22	3.46 (br t, *J*=6.0 Hz, 2H)	3.65–3.60 (m, 2H)
23	3.98 (dd, *J*=14.3, 4.2 Hz, 1H)	3.81 (dt, J=14.0, 4.6 Hz, 1H)
24	4.01 (s, 3H)	4.02 (s, 3H)
25	4.18 (ddd, *J*=15.5, 11.1, 4.9 Hz, 1H)	4.37 (td, *J*=9.1, 5.8 Hz, 1H)
26	4.29 (appar td, *J*=9.0, 5.7 Hz, 1H)	4.49 (t, *J*=9.0 Hz, 1H)
26′	4.31 (appar t, *J*=8.1 Hz, 1H)	
27	4.42 (d, *J*=8.7 Hz, 1H)	4.67 (dq, *J*=9.3, 7.1 Hz, 1H)
28	4.68 (dq, *J*=8.1, 6.9 Hz, 1H)	4.75 (d, *J*=8.3 Hz, 1H)
29	4.78 (ddd, *J*=8.4, 6.9, 5.5 Hz, 1H)	4.95 (td, *J*=8.4, 6.4 Hz, 1H)
30	6.25 (d, *J*=8.5 Hz, 1H)	5.94 (br s, 1H)
31	6.72 (br q, *J*=3.4 Hz, 1H)	6.91 (d, *J*=9.1 Hz, 1H)
32	6.90 (d, *J*=9.1 Hz, 1H)	6.94 (d, *J*=9.0 Hz, 1H)
33	7.05–7.04 (m, 2H)	7.07 (appar d, *J*=7.5 Hz, 2H)
34	7.09 (d, *J*=7.5 Hz, 2H)	7.12 (appar dd, *J*=7.4, 1.7 Hz, 2H)
35	7.20–7.16 (m, 3H)	7.23–7.17 (m, 3H)
36	7.25 (appar t, *J*=7.4 Hz, 1H)	7.32 (br q, *J*=4.4 Hz, 1H)
37	7.30 (appar t, *J*=7.6 Hz, 2H)	7.35 (appar t, *J*=7.4 Hz, 1H)
38	7.85 (br q, *J*=4.3 Hz, 1H)	7.41 (appar t, *J*=7.5 Hz, 2H)
39	8.09 (d, *J*=8.6 Hz, 1H)	8.18 (d, *J*=8.9 Hz, 1H)
40	8.34 (dd, *J*=9.0, 2.8 Hz, 1H)	8.36 (dd, *J*=9.0, 2.8 Hz, 1H)
41	8.52 (d, *J*=9.2 Hz, 1H)	8.72 (s, 1H)
42	8.58 (d, *J*=2.6 Hz, 1H)	8.78 (d, *J*=9.3 Hz, 1H)
43	10.01 (s, 1H)	10.41 (s, 1H)
44	10.86 (d, *J*=7.1 Hz, 1H)	11.02 (d, *J*=7.8 Hz, 1H)
45	11.03 (br d, *J*=5.3 Hz, 1H)	11.18 (d, *J*=6.5 Hz, 1H)

Spectra were recorded at 298 K in 25 mM $CDC1_3$ solution.

the efficiency of the data collection by allowing the purely antiphase cross peaks to come partially into phase, so that the cross peak multiplet has a non-zero integral.[29] In this way, fewer t_1 increments need be recorded before the cross peaks become discernible. The diagonal peaks gain some antiphase character by the same token, making them somewhat less intrusive, and allowing a milder filter function to be used. The bipolar gradients effectively cancel eddy-current effects, and avoid disturbing the field-frequency lock, making them ideal for very fast repetition rates.[30]

The Tr-ROESY sequence (Fig. 4b) was used to obtain information on spatial proximity as measured by cross relaxation.[21] This sequence gives phase-sensitive two-dimensional spectra by the usual method of States et al.[31] A mixing time τ_m=300 ms gave adequate cross peak intensity and only small COSY-type peaks arising from zero-quantum coherence in the rotating frame. As key contacts arise from spins with no *J* coupling, the small COSY-type peaks present little practical problem. Tables 2 and 3 summarize the one-dimensional reference spectra and Tr-ROESY NMR data from these studies.

Acknowledgements

This work was supported by the National Institutes of Health Grant GM-49076 and National Science Foundation Grant CHE-9813105. E. M. S. thanks the National Institute on Aging for support in the form of a training grant (National Research Service Award AG00096). J. S. N. thanks the following agencies for support in the form of awards: the Camille and Henry Dreyfus Foundation (Teacher–Scholar Award), the American Chemical Society

Table 3. ^{1}H NMR Tr-ROESY crosspeaks for artificial β-sheets **6**

Resonance	Artificial β-sheet **6a**	Artificial β-sheet **6b**
1	6 (s), 9 (m), 10 (s), 26 (s)	7 (s), 8 (s), 9 (s), 25 (s), 33 (w)
2	6 (s), 9 (s), 10 (s), 26 (m), 36 (w), 37 (m)	7 (s), 8 (s), 9 (s), 25 (m), 33 (w)
3	11 (s), 26′ (s), 29 (w), 30 (m), 41 (w)	11 (s), 26 (s), 32 (w), 34 (m), 35 (m), 42 (m)
4	11 (s), 26′ (s), 29 (m), 30 (s), 41 (w)	11 (s), 26 (s), 32 (s), 34 (m), 35 (m)
5	28 (s), 34 (w), 37 (w), 41 (m), 42 (m)	15 (m), 16 (s), 27 (s), 36 (w), 41 (m), 42 (s), 45 (w)
6	26 (w), 27 (w), 39 (w)	15 (m), 16 (s)
7	15 (m), 16 (s)	1 (s), 2 (s), 25 (m), 39 (m)
8	15 (m), 16 (s)	1 (s), 2 (s), 9 (s), 25 (m), 27 (m), 39 (m)
9	1 (m), 2 (s), 5 (w), 6 (w), 10 (m), 26 (m), 28 (m), 39 (m)	1 (s), 2 (s), 8 (s), 25 (m), 27 (m), 39 (w)
9′	N/a	10 (s), 19 (m), 21″ (m), 23 (m), 32 (m), 33 (w)
10	1 (s), 2 (s), 5 (w), 9 (m), 26 (m), 28 (m), 39 (w)	9′ (s), 18 (m), 19 (m), 23 (m), 32 (w)
11	3 (s), 4 (s), 26′ (s), 29 (w), 30 (s)	3 (s), 4 (s), 26 (m), 29 (m), 32 (s), 34 (m)
12	13 (s), 22 (s)	25 (w), 30 (s), 34 (w), 35 (m), 36 (m)
13	12 (s), 22 (s)	21′ (s), 22 (s)
14	31(s), 38 (w)	21′ (s), 22 (s)
15	7 (m), 8 (m), 38 (s)	5 (s), 6 (m), 35 (w), 36 (s)
16	7 (s), 8 (s), 45 (s)	5 (s), 6 (s), 45 (s)
16′	N/a	28 (s), 29 (s), 34 (s), 35 (w)
17	19′ (s), 27 (m), 29 (s), 33 (s)	28 (s), 29 (s), 34 (s), 35 (w)
18	23 (m), 25 (s)	10 (m), 21″ (s), 23 (m), 32 (s)
19	43 (m)	9′ (m), 10 (m), 23 (s), 33 (m)
19′	17 (s), 27 (m), 29 (s), 33 (s)	43 (m)
20	43 (m)	43 (m)
21	18 (m), 23 (s), 34 (m)	22′ (s), 43 (m)
21′	N/a	13 (s), 14 (s)
21″	N/a	9′ (m), 18 (s), 32 (s)
22	12 (s), 13 (s)	13 (s), 14 (s)
22′	N/a	21 (s), 43 (s)
23	18 (m), 21(s)	9′ (m), 10 (m), 18 (m), 19 (s), 33 (m)
24	32 (s), 44 (m)	31 (s), 44 (s)
25	18 (s), 30 (s)	1 (s), 2 (s), 7 (m), 8 (m), 9 (m), 30 (s), 39 (s)
26	1 (s), 2 (m), 6 (m), 9 (m), 10 (s), 31 (m), 39 (m)	3 (s), 4 (s), 11 (m), 32 (m), 41 (s), 42 (s)
26′	3 (s), 4 (s), 11 (s), 30 (m), 41 (s), 42 (s)	N/a
27	17 (m), 19′ (m), 33 (m), 34 (s), 39 (m)	5 (s), 8 (m), 9 (m), 36 (s), 39 (m), 42 (m)
28	3 (w), 5 (s), 9 (s), 10 (m), 26 (w), 38 (s), 39 (m), 41 (m)	16′ (s), 17 (s), 29 (s), 33 (s), 34 (m), 39 (w)
29	3 (m), 4 (m), 11 (w), 17 (s), 19′ (s), 27 (s), 30 (w), 33 (m), 39 (s)	11 (m), 16′ (s), 17 (s), 28 (s), 32 (w), 34 (s), 39 (s)
30	3 (m), 4 (s), 11 (m), 25 (s), 26′ (m), 34 (w)	12 (s), 25 (s), 39 (m)
31	14 (s), 26 (m)	12 (w), 24 (s), 40 (s)
32	24 (s), 40 (s)	3 (w), 4 (s), 9′ (m), 10 (w), 11 (s), 18 (s), 21″ (s), 26 (m), 29 (w)
33	1 (w), 3 (w), 4 (w), 17 (s), 19′ (s), 27 (s), 29 (s)	1 (s), 2 (m), 7 (w), 9′ (m), 10 (m), 18 (w), 19 (s), 23 (m), 28 (s), 29 (m), 37 (s), 38 (s)
34	2 (w), 5 (w), 21 (s), 27 (s), 30 (s), 39 (m)	3 (s), 4 (m), 11 (m), 12 (w), 16′ (s), 17 (s), 28 (m), 29 (s), 35 (s)
35	1 (m)	3 (m), 12 (m), 15 (m), 16′ (m), 17 (m), 29 (m), 30 (w), 34 (s)
36	2 (w)	5 (w), 12 (m), 15 (s), 27 (s)
37	2 (m), 5 (w)	29 (w), 33 (s)
38	14 (w), 15 (s), 28 (s)	1 (w), 2 (w), 29 (m), 33 (s)
39	6 (w), 9 (m), 10 (w), 26 (m), 27 (m), 28 (w), 29 (m), 34 (w)	7 (w), 8 (m), 9 (m), 25 (m), 27 (m), 28 (m), 29 (s), 30 (w)
40	32 (s)	31(s), 43 (w)
41	3 (w), 5 (m), 26′ (s), 28 (m)	5 (w), 26 (s), 43 (s)
42	5 (m), 26′ (s), 43 (s)	3 (m), 5 (s), 26 (s), 27 (m), 45 (w)
43	19 (m), 20 (m), 42 (s)	19′ (m), 20 (m), 21 (m), 22′ (s), 41 (s)
44	24 (m)	5 (w), 24 (m)
45	5 (w), 16 (m)	5 (w), 16 (m), 42 (w)

Spectra were recorded at 298 K in 25 mM $CDC1_3$ solution. Crosspeaks in the f_1 dimension are tabulated for each resonance in the f_2 dimension.

(Arthur C. Cope Scholar Award), and the Alfred P. Sloan Foundation (Alfred P. Sloan Research Fellowship).

References

1. (a) Mutter, M.; Altmann, E.; Altmann, K.-H.; Hersperger, R.; Koziej, P.; Nebel, K.; Tuchscherer, G.; Vuilleumier, S.; Gremlich, H.-U.; Müller, K. *Helv. Chem. Acta* **1988**, *71*, 835–847. (b) Mutter, M.; Vuilleumier, S. *Angew. Chem., Int. Ed. Engl.* **1989**, *28*, 535–554. (c) Tuchscherer, G.; Dörner, B.; Sila, U.; Kabmer, B.; Mutter, M. *Tetrahedron* **1993**, *49*, 3559–3575.
2. (a) Wagner, G.; Feigel, M. *Tetrahedron* **1993**, *49*, 10831–10842. (b) Brandmeier, V.; Sauer, W. H. B.; Feigel, M. *Helv. Chim. Acta* **1994**, *77*, 70–85.
3. (a) Kemp, D. S.; Bowen, B. R. *Tetrahedron Lett.* **1988**, *29*, 5077–5080. (b) Kemp, D. S.; Bowen, B. R. *Tetrahedron Lett.* **1988**, *29*, 5081–5082. (c) Kemp, D. S.; Bowen, B. R.; Muendel, C. C. *J. Org. Chem.* **1990**, *55*, 4650–4657. (d) Kemp, D. S.; Li, Z. Q. *Tetrahedron Lett.* **1995**, *36*, 4175–4178.
4. (a) Diaz, H.; Tsang, K. Y.; Choo, D.; Espina, J. R.; Kelly, J. W. *J. Am. Chem. Soc.* **1993**, *115*, 3790–3791. (b) Tsang, K. Y.; Diaz, H.; Graciani, N.; Kelly, J. W. *J. Am. Chem. Soc.* **1994**, *116*, 3988–4005. (c) Nesloney, C. L.; Kelly, J. W.

J. Am. Chem. Soc. **1996**, *118*, 5836–5845. (d) Bekele, H.; Fendler, J. H.; Kelly, J. W. *J. Am. Chem. Soc.* **1999**, *121*, 7266–7267. (e) Lashuel, H. A.; LaBrenz, S. R.; Woo, L.; Serpell, L. C.; Kelly, J. W. *J. Am. Chem. Soc.* **2000**, *122*, 5262–5277.

5. For a review, see: Gellman, S. H. *Acc. Chem. Res.* **1998**, *31*, 173–180.
6. (a) Krauthäuser, S.; Christianson, L. A.; Powell, D. R.; Gellman, S. H. *J. Am. Chem. Soc.* **1997**, *119*, 11719–11720. (b) Chung, Y. J.; Christianson, L. A.; Stanger, H. E.; Powell, D. R.; Gellman, S. H. *J. Am. Chem. Soc.* **1998**, *120*, 10555–10556. (c) Chung, Y. J.; Huck, B. R.; Christianson, L. A.; Stanger, H. E.; Krauthäuser, S.; Powell, D. R.; Gellman, S. H. *J. Am. Chem. Soc.* **2000**, *122*, 3995–4004. (d) Fisk, J. D.; Powell, D. R.; Gellman, S. H. *J. Am. Chem. Soc.* **2000**, *122*, 5443–5447. (e) Fisk, J. D.; Gellman, S. H. *J. Am. Chem. Soc.* **2001**, *123*, 343–344.
7. For a review, see: Seebach, D.; Matthews, J. L. *Chem. Commun.* **1997**, 2015–2022.
8. (a) Seebach, D.; Abele, S.; Gademann, K.; Jaun, B. *Angew. Chem., Int. Ed. Engl.* **1999**, *38*, 1595–1597. (b) Daura, X.; Gademann, K.; Schäfer, H.; Jaun, B.; Seebach, D.; van Gunsteren, W. F. *J. Am. Chem. Soc.* **2001**, *123*, 2393–2404.
9. For reviews, see: (a) Smith, C. K.; Regan, L. *Acc. Chem. Res.* **1997**, *30*, 153–161. (b) Gellman, S. H. *Curr. Opin. Chem. Biol.* **1998**, *2*, 717–725. (c) Lacroix, E.; Kortemme, T.; de la Paz, M. L.; Serrano, L. *Curr. Opin. Struct. Biol.* **1999**, *9*, 487–493.
10. (a) Sharman, G. J.; Searle, M. S. *Chem. Commun.* **1997**, 1955–1956. (b) Doig, A. J. *Chem. Commun.* **1997**, 2153–2154. (c) Schenck, H. L.; Gellman, S. H. *J. Am. Chem. Soc.* **1998**, *120*, 4869–4870. (d) Das, C.; Raghothama, S.; Balaram, P. *J. Am. Chem. Soc.* **1998**, *120*, 5812–5813. (e) Kortemme, T.; Ramírez-Alvarado, M.; Serrano, L. *Science* **1998**, *281*, 253–256. (f) Das, C.; Raghothama, S.; Balaram, P. *Chem. Commun.* **1999**, 967–968. (g) de Alba, E.; Santoro, J.; Rico, M.; Jimenez, M. A. *Protein Sci.* **1999**, *8*, 854–865. (h) Das, C.; Nayak, V.; Raghothama, S.; Balaram, P. *J. Peptide Res.* **2000**, *56*, 307–317. (i) Griffiths-Jones, S. R.; Searle, M. S. *J. Am. Chem. Soc.* **2000**, *122*, 8350–8356.
11. Nowick, J. S.; Smith, E. M.; Noronha, G. *J. Org. Chem.* **1995**, *60*, 7386–7387.
12. (a) Nowick, J. S.; Holmes, D. L.; Mackin, G.; Noronha, G.; Shaka, A. J.; Smith, E. M. *J. Am. Chem. Soc.* **1996**, *118*, 2764–2765. (b) Nowick, J. S.; Pairish, M.; Lee, I. Q.; Holmes, D. L.; Ziller, J. W. *J. Am. Chem. Soc.* **1997**, *119*, 5413–5424. (c) Smith, E. M.; Holmes, D. L.; Shaka, A. J.; Nowick, J. S. *J. Org. Chem.* **1997**, *62*, 7906–7907. (d) Tsai, J. H.; Waldman, A. S.; Nowick, J. S. *Bioorg. Med. Chem.* **1999**, *7*, 29–38.
13. Nowick, J. S.; Mahrus, S.; Smith, E. M.; Ziller, J. W. *J. Am. Chem. Soc.* **1996**, *118*, 1066–1072.
14. Nowick, J. S.; Cary, J. M.; Tsai, J. H. *J. Am. Chem. Soc.* **2001**, *123*, 5176–5180.
15. For preliminary accounts of these studies, see: (a) Holmes, D. L.; Smith, E. M.; Nowick, J. S. *J. Am. Chem. Soc.* **1997**, *119*, 7665–7669. (b) Nowick, J. S. *Acc. Chem. Res.* **1999**, *32*, 287–296.
16. Nowick, J. S.; Powell, N. A.; Martinez, E. J.; Smith, E. M.; Noronha, G. *J. Org. Chem.* **1992**, *57*, 3763–3765.
17. Nowick, J. S.; Abdi, M.; Bellamo, K. A.; Love, J. A.; Martinez, E. J.; Noronha, G.; Smith, E. M.; Ziller, J. W. *J. Am. Chem. Soc.* **1995**, *117*, 89–99.
18. We have, unfortunately, never been able to crystallize any of our artificial β-sheets.
19. We have also synthesized artificial β-sheet **6a** using solid-phase methods. For a description, see Ref. 15a.
20. (a) Nowick, J. S.; Holmes, D. L.; Noronha, G.; Smith, E. M.; Nguyen, T. M.; Huang, S.-L. *J. Org. Chem.* **1996**, *61*, 3929–3934. (b) Nowick, J. S.; Holmes, D. L.; Noronha, G.; Smith, E. M.; Nguyen, T. M.; Huang, S.-L.; Wang, E. H. *J. Org. Chem.* **1998**, *63*, 9144.
21. (a) Hwang, T. L.; Shaka, A. J. *J. Am. Chem. Soc.* **1992**, *114*, 3157–3159. (b) Hwang, T. L.; Shaka, A. J. *J. Magn. Reson., Ser. B* **1993**, *102*, 155–165.
22. The older version of the AMBER* force field associated with this version of MacroModel appears to better reproduce the preference of the diacylhydrazine groups of **6a** and **6b** to adopt a linear conformation, which is evidenced by the large $^3J_{HNNH}$ coupling constants in their ^{1}H NMR spectra.
23. Wüthrich, K. *NMR of Proteins and Nucleic Acids*; Wiley: New York, 1986 pp 125–129.
24. Wüthrich, K. *NMR of Proteins and Nucleic Acids*; Wiley: New York, 1986 pp 166–168.
25. This concentration (1.0 mM) provides adequate signal-to-noise ratio without significant self-association. Studies of the concentration dependence of the chemical shifts of the NH groups of **6a** from 0.5–200 mM and **6b** from 0.3–89 mM in $CDCl_3$ reveal negligible self-association ($K_{assoc} \leq 1\ M^{-1}$) at the concentrations used for both the chemical shift and the NOE studies in this paper.
26. This comparison should be interpreted with caution, because the shift differences are small (several tenths of a ppm) and are only slightly greater than the few tenths ppm downfield shifting that occurs to an amide or urea NH group when its carbonyl group accepts a hydrogen bond (e.g. H_h or H_a in Chart 3).
27. Dueholm, K. L.; Egholm, M.; Buchardt, O. *Org. Prep. Proc. Int.* **1993**, *25*, 457–461.
28. Hurd, R. E. *J. Magn. Reson.* **1990**, *87*, 422–428.
29. Bax, A.; Freeman, R. *J. Magn. Reson.* **1981**, *44*, 542–561.
30. Wider, G.; Wüthrich, K. *J. Magn. Reson., Ser. A* **1994**, *108*, 255–258.
31. States, D. J.; Haberkorn, R. A.; Ruben, D. J. *J. Magn. Reson.* **1982**, *48*, 286–292.